Earthq Eng & Eng Vib (2016) 15: 743-757 **DOI**: 10.1007/s11803-016-0362-9

Prediction of seismic collapse risk of steel moment frame mid-rise structures by meta-heuristic algorithms

Fooad Karimi Ghaleh Jough[1†] and Serhan Şensoy[2‡]

1. *Department of Civil Engineering, Sarab Branch, Islamic Azad University, Sarab, Iran*

2. *Department of Civil Engineering, Eastern Mediterranean University, Gazimagusa, Mersin10, Turkey*

Abstract: Different performance levels may be obtained for sideway collapse evaluation of steel moment frames depending on the evaluation procedure used to handle uncertainties. In this article, the process of representing modelling uncertainties, record to record (RTR) variations and cognitive uncertainties for moment resisting steel frames of various heights is discussed in detail. RTR uncertainty is used by incremental dynamic analysis (IDA), modelling uncertainties are considered through backbone curves and hysteresis loops of component, and cognitive uncertainty is presented in three levels of material quality. IDA is used to evaluate RTR uncertainty based on strong ground motion records selected by the k-means algorithm, which is favoured over Monte Carlo selection due to its time saving appeal. Analytical equations of the Response Surface Method are obtained through IDA results by the Cuckoo algorithm, which predicts the mean and standard deviation of the collapse fragility curve. The Takagi-Sugeno-Kang model is used to represent material quality based on the response surface coefficients. Finally, collapse fragility curves with the various sources of uncertainties mentioned are derived through a large number of material quality values and meta variables inferred by the Takagi-Sugeno-Kang fuzzy model based on response surface method coefficients. It is concluded that a better risk management strategy in countries where material quality control is weak, is to account for cognitive uncertainties in fragility curves and the mean annual frequency.

Keywords: modelling uncertainty; cognitive uncertainty; TSK model; Cuckoo algorithm

1 Introduction

Collapse is one of the main reasons for loss of life and property during an earthquake. Earthquakes cause serious damage by destroying buildings and/or rendering them unsafe and unusable (Kircher *et al*., 1997). Quantifying earthquake damage has become a serious research topic. Structures may collapse in two ways: The first one is sideway collapse, which results in the loss of lateral stability. Sideway collapse is itself the result of incremental and consecutive losses of capacity by the structural elements which comprise the load-resisting system. In contrast, vertical collapse, the second way of collapse, is the result of direct loss of components which contribute to the gravitational stability of the structure (Zareian *et al*., 2009).

Structural uncertainties include mainly the uncertainties associated with the earthquake (record to record uncertainty), the uncertainties associated with the model (modelling uncertainty), and those associated with materials (cognitive uncertainty). Record to Record (RTR) uncertainties stem from the random nature of seismic activity and the lack of knowledge about deep geological causes. Modelling uncertainty is part and parcel of modelling itself; discrepancies exist between a model and the actual data collected on a phenomenon (Liel *et al*., 2009). The third source of uncertainty is also of prime importance especially in countries where supervision is not very rigorous.

There are two important relations in seismic assessment of structures: The first one is between intensity measure (IM) and the collapse probability or fragility, and the second is between the hazard curve and IM (Zareian *et al*., 2009). The effects of each of a number of parameters e.g., material quality (Dimova and Negro, 2006), irregular story (Kappos and Panagopoulos, 2010), and building height (Erberik, 2008), have been considered by various researchers in determining the fragility curves. Rajeev and Tesfamariam (2012) have considered interactions among the parameters such as irregularities (weak story, irregular story, vertical discontinuities etc.,) and material quality to develop fragility curves. Liel *et al*. (2009) has presented the effect of modelling uncertainty in collapse limit state in comparison with other limit state such as immediate occupancy and life safety in fragility curves. Zareian *et al*. (2009) incorporated RTR variability and modelling

Correspondence to: Fooad Karimi Ghaleh Jough, Department of Civil Engineering, Sarab Branch, Islamic Azad University, Sarab, Iran
Tel: +98 (914) 5353339
E-mail: karimi@iausa.ac.ir
†Assistant Professor; ‡Associate Professor
Received May 5, 2015; **Accepted** August 31, 2015

uncertainties through the incremental dynamic analysis (IDA) on deriving the fragility curves. Fuzzy logic is used for risk analysis, safety evaluation and structural analysis to incorporate the impact of modelling uncertainty (Rajeev and Tesfamariam, 2012; Möller *et al*., 2003).

This study investigates the effect of cognitive uncertainties in material quality versus modelling uncertainties in quantifying fragility curves for sideway collapse limit state of structures by using the Cuckoo algorithm and the Takagi-Sugeno-Kang (TSK, Sugeno, 1985) model. IDA is applied to consider RTR uncertainty with strong ground motion records selected by the k-means algorithm, which reduces calculation time compared with methods that involve random sampling. At the structural level four meta variables viz. beam strength (BS), column strength (CS), beam ductility (BD) and column ductility (CD) are considered for defining modelling uncertainty. RTR and modelling uncertainties are incorporated through the response surface method (RSM). Analytical equations of RSM are obtained through IDA results by the Cuckoo algorithm, which predicts the mean and standard deviation (SD) of the collapse fragility curve. Three levels of material quality (MQ) are predicted for different levels of cognitive uncertainty. The TSK model is used for MQ uncertainties by the response surface coefficients. Finally collapse fragility curves with various sources of uncertainties are derived through a large number of MQ values and meta variables inferred by the TSK system based on RSM coefficients.

As demonstration of the efficiency of the method the procedure is applied to a five-story moment resistant frame and a ten-story counterpart. Figure 1 depicts the uncertainties considered in this study. It is expected that the methodology, with special attention paid to cognitive uncertainties, will enhance seismic performance assessment of large building stock in regions that lack quality control of materials.

2 Combination of sources of uncertainty

The main step in predicting the effect of modelling uncertainty is to combine various uncertainties such as RTR with the modelling uncertainties. In this effort, RTR, modelling and cognitive are considered as separate uncertainties (Kiureghian and Ditlevsen, 2009). Three common methods to incorporate the effects of RTR and modelling uncertainties are confidence interval, mean estimate and Monte Carlo simulation (Cornell *et al*., 2002; Ellingwood and Kinali, 2009). In the mean estimate method, the mean value of the fragility curves remained unchanged while the variance which reflects modelling uncertainties varies. In contrast, the confidence interval approach considers the variance of fragility curve unchanged.

Results obtained by this method are not sensitive to a particular class of uncertainties and in fact classes are not explicit in the results. The Monte Carlo method implements thousands of simulations for modelling parameter values based on their probabilistic distributions and samples are analysed based on the simulated values as modelling parameters of the structure. Thousands of collapse fragility curves, i.e., the probability of collapse versus intensity measure values, that include the effects of modelling uncertainties result from this accurate analysis (Liel *et al*., 2009). In recent studies (Seo and Linzell, 2013), a new approach to consider modelling uncertainty combines the Monte Carlo method with the RSM. Since the Monte Carlo simulation approach requires a large number of simulations in order to

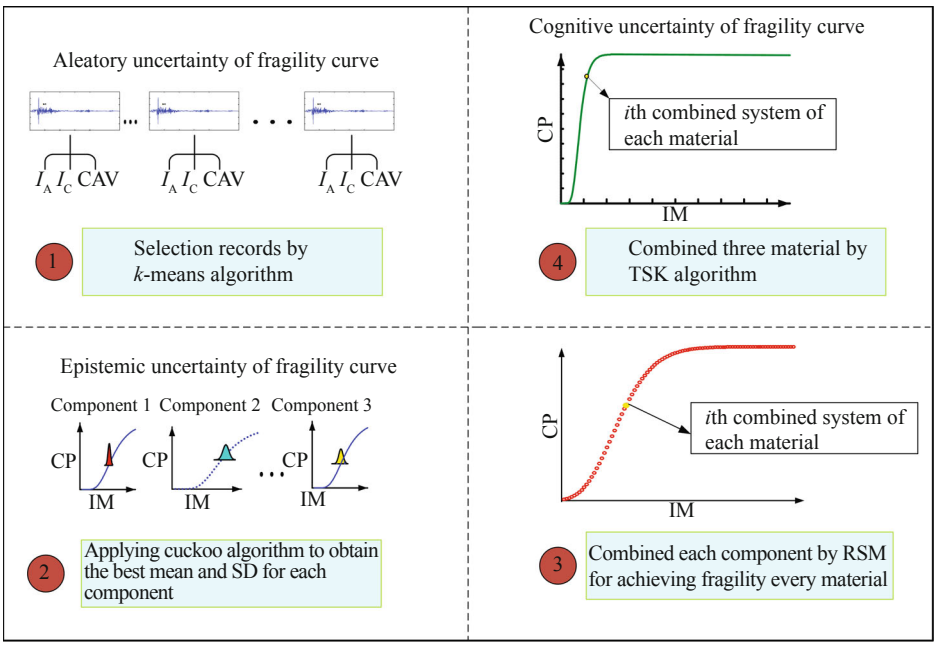

Fig. 1 Uncertainty analysis of the system fragility curve by RSM and TSK method

incorporate various uncertainties, RSM helps to bring the computation cost down to an affordable level. RSM in combination with Monte Carlo simulation is used for seismic vulnerability assessment of horizontally curved steel bridges (Seo and Linzell, 2012), concrete building structures (Liel *et al*. 2009; Franchin *et al*. 2003) and steel framed structures (He and Wang, 2011). Also, RSM has been applied in previous relevant literature to derive fragility curves (Rajeev and Tesfamariam, 2012; Rossetto and Elnashai, 2005; Schotanus *et al*., 2004). The initial in this approach is to conduct a sensitivity analysis to determine which modelling parameter contributes the most to the mean and standard deviation (SD) of fragility. Then, regression analysis is used to compile the fragility curve based on an analysis of sensitivity. To this end, the second order polynomial function given in Eq. (1) is used for the estimation of the mean and SD (using Monte Carlo method) for different scenarios of modelling uncertainty. Results obtained using the Monte Carlo method conform with estimates obtained from a variety of models (Seo and Linzell, 2013).

$$y = \beta_0 + \sum_{i=1}^{k} \beta_i x_i + \sum_{i=1}^{k} \beta_i x_i^2 + \sum_{i=1}^{k-1} \sum_{j>i}^{k} \beta_{ij} x_i x_j \tag{1}$$

In this study, the *k*-means algorithm is used to select records that constitute RTR uncertainty. Then the Cuckoo algorithm is used to derive the mean and SD of each defined scenario of modelling uncertainty. Finally the TSK algorithm is used to incorporate cognitive uncertainty. The three algorithms are defined as follows.

2.1 RTR uncertainty

Much data are needed for a full definition of strong ground motion because the phenomena are relatively complicated. IM is the summary of a number of ground motion variables that simplifies the definition of an earthquake and at the same time connects seismic hazard with structural damage. The most important properties of ground motion are: Arias intensity (I_A) that reflects amplitude, characteristic intensity (I_C) that shows the frequency content, and cumulative absolute velocity (CAV) that portends the potential to damage buildings by calculating the duration of records. Arias intensity (I_A) is described as Eq. (2)

$$I_A = \frac{\pi}{2g} \int_0^{\infty} \left[a(t)^2 \right] \mathrm{d}t \tag{2}$$

where $a(t)$ is the acceleration intensity and the unit of (I_A) is meter per second. The infinity symbol in the equation indicates that I_A is calculated based on whole duration and not T_d (duration of the record).

Characteristic intensity (I_C) is described as

$$I_C = \alpha_{rms}^{1.5} T_d^{0.5}, \quad \infty_{rms} = \frac{1}{t_d} \int_0^{t_d} \left[a(t)^2 \right] \mathrm{d}t \tag{3}$$

Cumulative absolute velocity (CAV) is the continuous accumulation of acceleration during the earthquake and it is calculated by the following Eq. (4)

$$\mathrm{CAV} = \int_0^{T_d} |a(t)| \mathrm{d}t \tag{4}$$

CAV is the best parameter relating to structural damage for various earthquake disasters (Kramer, 1996).

RTR uncertainty is considered through the IDA approach. Selecting the ground motion is the main step in applying the IDA method for considering the effects of RTR uncertainty. In this paper, the *k*-means algorithm is used to decrease the dispersion of uncertainty and facilitate proper selection of ground motion.

First, one hundred records of natural earthquakes are selected by site specification according to following properties:

- Records obtained in the region with longitude 124°–115° and latitude 32°–41°;
- Moment magnitude (M_w) greater than 5;
- Minimum epicentral distance (R) 150 km.

To further prune this collection we used the *k*-means algorithm since random selection of data from the group may cause dispersion of results.

2.1.1 Lloyd's algorithm (*k*-means algorithm)

Proper selection of earthquake records may be performed through different steps such as classification and clustering. Classification is supervised learning; training data are needed. Clustering is unsupervised, requiring no training data. Generally speaking, classification is used to assign defined tag to samples according to the basic features, and clustering is used to categorize similar samples on the basic features and does not assign to every group. Lloyd's algorithm (Lloyd, 1982) is an unsupervised clustering algorithm. At the beginning of the analysis, the number of clusters *k* and the centroid of center (COC) of each clusters are determined. Any sample can be taken randomly or the first *k* samples in sequence as the initial centroids. The steps in Lloyd's algorithm are as follows:

- Decide the centroid point
- Decide the distance of each sample to the centroid (see Eq. (5))
- Categorize the sample based on optimum distance

$$D = \sum_{j=1}^{k} \sum_{i=1}^{n} \| x_i^j - c_j \|^2 \tag{5}$$

where $\| x_i^j - c_j \|$ is a selected distance value between a data sample x_i^j and the cluster center c_j. D is then an index of the distance of n data samples from their relative cluster centers (Lloyd, 1982).

2.2 Modelling uncertainty

In the IM-based (vertical statistics format) approach (Mitropoulou and Papadrakakis, 2011), seismic fragility curves are shown as:

$$P\left(\mathrm{Collapse}|\mathrm{IM} = \mathrm{im}_i\right) = P\left(\mathrm{im}_i > \mathrm{IM}_{\mathrm{collapse}}\right) = F_{\mathrm{IM}_{\mathrm{collapse}}(\mathrm{im}_i)} \tag{6}$$

According to (Shinozuka *et al*., 2000), it is presumed that two-value (mean-η and log-SD-β) lognormal distribution functions could define the curves F_R and the maximum likelihood approach used to estimate the two parameters. The likelihood function for the present purpose is defined as follows:

$$L\left(\eta_1,\eta_2,\ldots,\eta_n,\beta_1,\beta_2,\ldots,\beta_n\right)=\prod_{i=1}^{N}F_{\mathrm{R}}\left(S_{\mathrm{A},i},y_k\right) \quad (7)$$

where F_{R} denotes the seismic fragility curve for collapse limit state, $S_{\mathrm{A},i}$ is the intensity measure value to which the i-th scenario of the sample is considered, N is the number of sample scenarios. Therefore, F_{R} has the following form:

$$F_{\mathrm{R}}=\Phi\left[\frac{\ln(\mathrm{im}_i/\eta_{\ln(\mathrm{im}_c)})}{\beta_{\ln(\mathrm{im}_c)}}\right] \quad (8)$$

In Eq. (8), η is the mean and β is the SD of the collapse probability function and ϕ is the normal distribution function. It is clear that both the mean and SD values of a collapse fragility curve are affected when modelling uncertainty is involved. The modelling uncertainty is considered ±1.7 β away from the mean and ±1 β with correlation of each of the meta variables BD, BS, CS and CD. The two parameters η and β are evaluated by maximizing ln (L), and in this study the Cuckoo optimization algorithm is used.

2.2.1 Cuckoo optimization algorithm

The optimization algorithm used to solve the 2n-value (η, β) problem maximizing ln (L) is the Cuckoo (CO) algorithm because it is obvious that the number of variables for CO is less than that for GA (genetic algorithm) and PSO (particle swarm optimization), which are more suited for larger optimization problems. The CO optimization algorithm is a population-based method. To start, the matrix of $N_{\mathrm{p}}\times N_{\mathrm{var}}$ as candidate habitat is created to show the maximum number of cuckoos. Laying eggs from their habitats in a maximum distance is another habitat of real CO. Egg laying radius (ELR) is computed based on the Eq. (9), which represents the maximum limit (Rajabioun, 2011).

$$\mathrm{ELR}=\omega\times\frac{\text{Number of current cuckoo's eggs}}{\text{Total number of eggs}}\times\left(\mathrm{par}_h-\mathrm{par}_l\right) \quad (9)$$

where ω is an integer parameter, defined to apply the maximum value of ELR, par_h and par_l rameters, respectively. Each CO starts egg laying in the bird's nests randomly. After the egg laying step, S% (usually 10%–15%) of all eggs, with low benefit values, will be detected and destroyed. It is very amazing that only one egg can live in each nest. When COs grow, they begin living in their own community. During the egg laying period, the young COs migrate to new areas, while eggs are similar to host birds. The society with the high benefit value is chosen as the target point for other COs to migrate to after the CO groups are formed in various environment. The procedure of new egg laying is defined in Eq. (10) (Shokri-Ghaleh and Alfi, 2014)

$$X_{\mathrm{NextHabitat}}=X_{\mathrm{currentHabitat}}+F\left(X_{\mathrm{GoalPoint}}-X_{\mathrm{currentHabitat}}\right) \quad (10)$$

Here, X and F are the position and the motion coefficient, respectively. Figure 2 gives the pseudo-code of the CO algorithm.

2.3 Theory of inference in a fuzzy expert system (cognitive uncertainty)

Lotfi Zadeh (Sugeno, 1985) created fuzzy logic to present a way to map qualitative knowledge into mathematical reasoning. A fuzzy inference system is an expert knowledge-based (KB) system which contains fuzzy algorithms in a simple rule base. In this system the knowledge which is encoded in the rule base is emanated from human experience and intuition and the rules show the relationships between the inputs and outputs of a

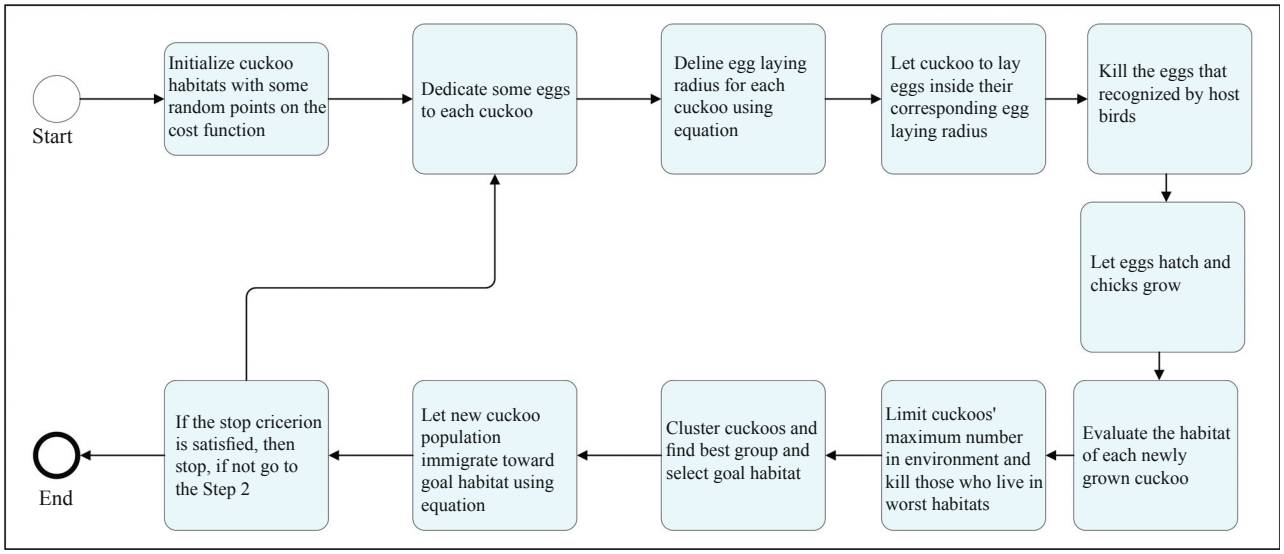

Fig. 2 The pseudo code representation of the Cuckoo algorithm

system. Numerical value of a linguistic variable (i.e. MQ in this study) could be presented by a fuzzy number. A FIS (fuzzy inference system) consists of four parts: fuzzifier, inference engine, KB, and defuzzification of results (see Fig. 3). Fuzzifier does the conversion of real numbers of input into fuzzy sets and defuzzification denotes the opposite action. The knowledge base consists of a database and a rule base. The database includes membership functions of the fuzzy sets, while the rule base includes a set of linguistic statements in the form of IF-THEN rules that are connected by AND operator while other operators such as OR, and NOT may also be used. The inference engine which forms the core of a fuzzy inference system uses IF-THEN rules contained in the rule base to find the output through fuzzy or approximate reasoning. The approximate reasoning process is to create conclusion from a set of IF-THEN rule. The Sugeno type (also known as the TSK fuzzy model) of FIS is written as follows:

R_i: *IF x is A AND y is B ... THEN* $z = ax+by+c$ $i = 1, 2,...,N$

in which the rule is shown as R_i, x and y are the parameters and A is the fuzzy set based on x, y. a and b are constants and N is the number of rules (Siler and Buckley, 2005). The centre of area (COA) is the most popular defuzzification approach in the Mamdani-type FIS. In Sugeno-type FIS, the final output is measured by the weighted average of all outputs (shown by Eq. (11)).

$$t = \frac{\sum_{i=1}^{N} w_i z_i}{\sum_{i=1}^{N} w_i} \tag{11}$$

$$w_i = \min\left(f_1(x_i), f_1(y_i), ...\right) \quad i = 1,2, ..., N \tag{12}$$

in which, w_i is the firing strength of rule i and is described by Eq. (12) and $f_1(x)$ are $f_1(y)$ membership functions of variable x and y, respectively. Since the target of FIS in this work is to predict coefficients of the response surfaces and are numerical variables, the Sugeno inference system is used.

3 Consideration of various uncertainties in study structures

3.1 Design of structure

To assess the effect of cognitive uncertainty on medium-rise steel buildings, one 5 story structure and a 10 story structure are assumed situated in a very high risk environment. It is further assumed that the soil on which these structures are situated is Type 2 soil (shear wave velocity between 360 to 750 m/s) (Stand No. 2800, 2007). The structures have regular plans (Fig. 4) with three 5 meter bays on each side and 3.2 meter floor height (Fig. 5). Floors are assumed to be rigid diaphragms with dead load distributions similar to what we normally see in structures in Iran and in accordance with Iranian

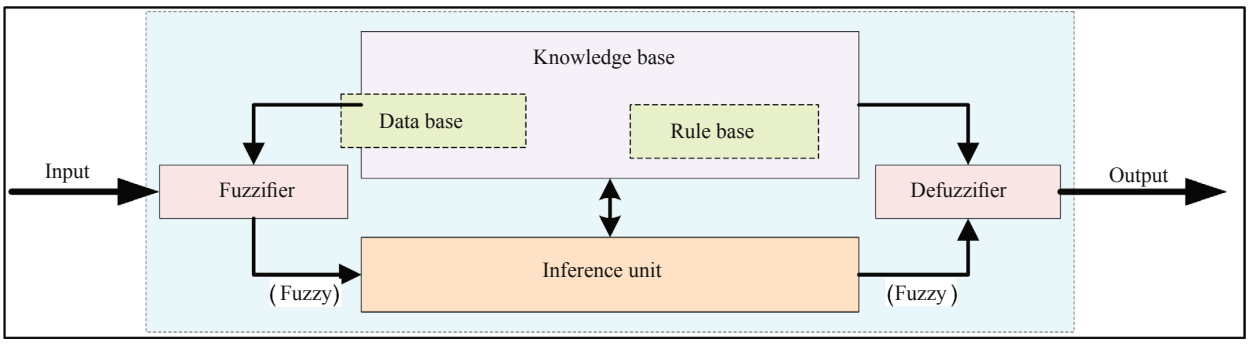

Fig. 3 Fuzzy expert systems perform fuzzy reasoning

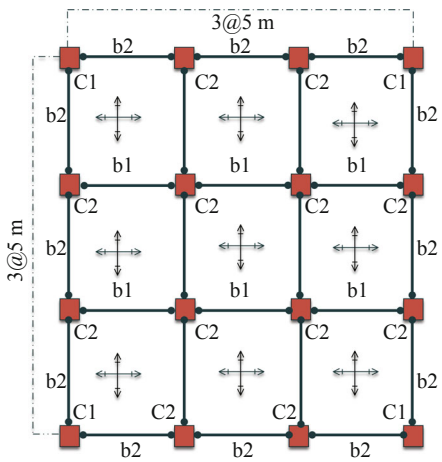

Fig. 4 The plan of sample structures

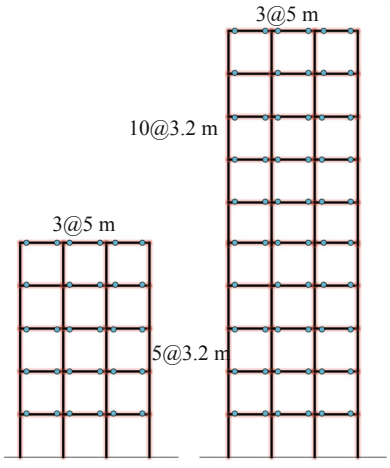

Fig. 5 Elevations view of samples

Seismic Code (Stand No, 2800; 2007), the response modification factor (i.e. R) is 7 for the sample structures. The nominal yield strength of steel is 240 MPa. Table 1 shows cross sections for all members.

Numerical modelling of a sample interior frame is implemented using the OpenSEES (2006) finite element program. For modelling uncertainty, nonlinear springs of the Ibara-Krawinkler (Liel *et al*., 2009) model are used, and lumped plastic hinges of columns, beams and panel zones are incorporated in the model for the same purpose (Liel *et al*., 2009). The backbone curve of the moment-rotation model is represented in Fig. 6. The element backbone is described by the following variables: yield strength (M_y), post yield strength (M_c), plastic rotation capacity (θ_p), post-capping plastic rotation (θ_{pc}), ultimate rotation capacity (θ_u) and cyclic deterioration (λ). θ_p, θ_{pc} and λ are the ductility variables.

The hysteretic behavior of a connection is described based on deterioration rules that are defined according to the energy dissipated in each hysteretic cycle. The deterioration of basic strength, post capping strength, unloading stiffness and reloading stiffness are represented in the model (Liel *et al*., 2009). Capacity of energy dissipation of the component, by which deterioration rules are formulated, is described as Eq. (13)

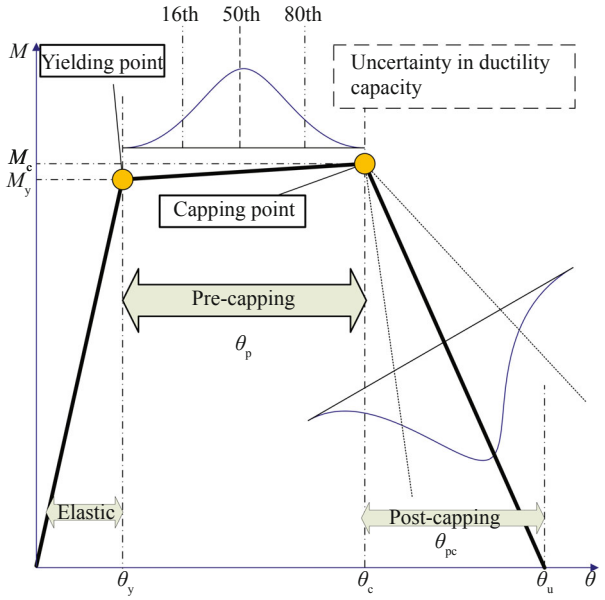

Fig. 6 Backbone curve of moment rotation model based on modified Ibarra-Medina-Krawinkler

$$E_t = \lambda \times M_y \tag{13}$$

where λ is the rate of cyclic deterioration and is based on calibration of experimental outcomes. Comparison of including and neglecting cyclic deterioration of component behaviour is given in Fig. 7.

The model variables are summarized in Table 2 and they are assumed to follow lognormal distributions with means and SD shown (Lignos, 2008). The ratio of (M_c/M_y) is the strength variable. As mentioned, the four meta random variables are beam strength (BS) (i.e. M_c/M_y for beams), column strength (CS) (i.e. M_c/M_y for columns), beam ductility (BD), (i.e. θ_p, θ_{pc} and λ for beams) and column ductility (CD) (i.e. θ_p, θ_{pc} and λ for columns), which represent strength and ductility for each element (Liel *et al*., 2009). No uncertainties are assumed for the panel zones because the structures are designed based on new guidelines which assume that rupture occurs first in the beams and not in the joints.

The proposed model as applied to an interior frame, M2-WO panel zone model, presented in Fig. 8 (Foutch and Yun, 2002).

3.2 Numerical tests

In the first mode, acceleration is assumed to be a measure of intensity ($S_a(T_1)$). This IM is used in different research and is represented to accomplish sufficiency and efficiency criteria in the prediction of structural damage, which is the main target in this work. Intersory drift ratio is selected as the engineering demand variable since it shows global behavior of the structure, which has good correlation with global collapse. Mean and (SD) of the modelling variables are affected by the quality of material. Low material quality leads to lower mean value and higher dispersion (Li and Ellingwood, 2008). Three levels of material quality (good-average-low) are considered. Experimental values (Mean and SD) are unchanged for good MQ. The mean value is decreased 25% and 40% for average MQ and Low MQ, respectively, while SD is increased 25% and 40% for average and low MQ, respectively, with respect to the value for good MQ. This pattern was used in previous investigations (Rajeev and Tesfamariam, 2012).

Consequently, we have four main meta variables (Pinto *et al*., 2007) and 33 combinations of these meta variables (hence 33 scenarios) are used for the sensitivity analysis and IDA. Eight of these scenarios correspond to

Table 1 Design properties for 5- and 10-story buildings

	Story	C1	C2	b1	b2
5-Story	1,2	TUBO 180×180×20	TUBO 300×300×20	IPE 450	IPE 330
	3,4,5	TUBO 160×160×20	TUBO 200×200×20	IPE 400	IPE 300
10-Story	1,2	TUBO 240×240×20	TUBO 400×400×20	IPE 500	IPE 400
	3,4,5,6	TUBO 220×220×20	TUBO 340×340×20	IPE 500	IPE 400
	7,8,9,10	TUBO 180×180×15	TUBO 280×280×20	IPE 400	IPE 360

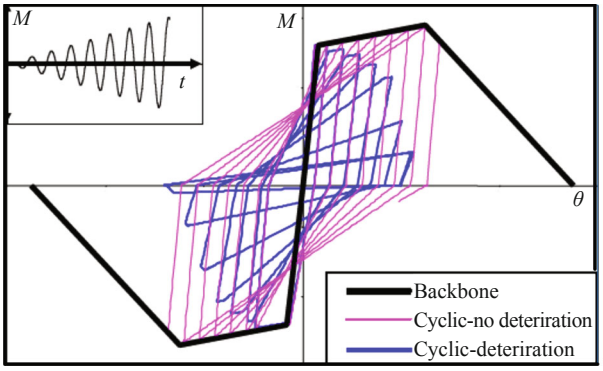

Fig. 7 Effects of cyclic deterioration modelling on *M-θ* backbone curves

only one variable and the other 25 scenarios correspond to interaction of variables taken two at a time. In the eight scenarios where one main meta variable is counted, its value is set at ±1.7 times the SD from the mean. In the other scenarios, the value of each main meta variable is set at ±1 SD from the mean. In general, (33×3×2) IDA analyses have been conducted on the 40 selected records selected by the k-means approach. The Hunt & Fill tracing algorithm (Vamvatsikos, 2007) is applied to scale the records in the IDA analyses to achieve good performance. In the *k*-means approach, first the COC is calculated in four clusters and then each cluster is defined based on records occurring near the COC based on the similarity of three parameters of the earthquake records. Finally, 10 records are selected from each cluster randomly. This procedure lower the desperation of samples. Figure 9 shows the position of each sample for every cluster in 3-D which is presented in appendix. Figure 10 shows the IDA curves for different quality levels of building material for the sample structure. The effect of the quality of building material on fragility is quite obvious.

3.3 Sensitivity analysis

With reference to the description of the meta variables, sensitivity analyses are performed to determine the effects of each parameter of the variables in various quality (MQ). Results of the sensitive analysis for sideways collapse of the sample 5-story structure are presented in Fig. 11, where Fig. 11 (a), (b) and (c) present created tornado diagrams of sensitivity outcomes and Fig. 11 (d) and (e) show results of histogram of the sensitivity analyses for each MQ. As depicted in the histogram dispersion for good material quality, structural

Table 2 Model parameters for beams and columns in uncertainty analysis

Random variable		Mean	Standard deviation
Beam	θ_p	0.025	0.43
	θ_{pc}	0.16	0.41
	λ	1.00	0.43
	M_c/M_y	1.11	0.05
column	θ_p	0.011	0.57
	θ_{pc}	0.07	0.92
	λ	0.4	0.96
	M_c/M_y	1.11	0.05

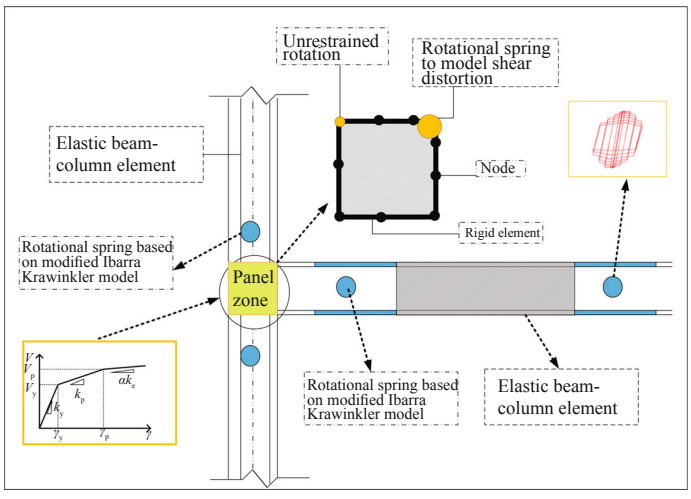

Fig. 8 M2-WO panel zone

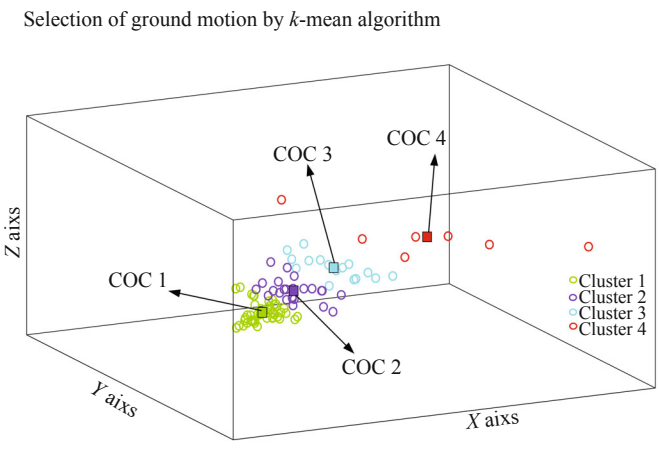

Fig. 9 *k*-means sampling in the three-dimensional space

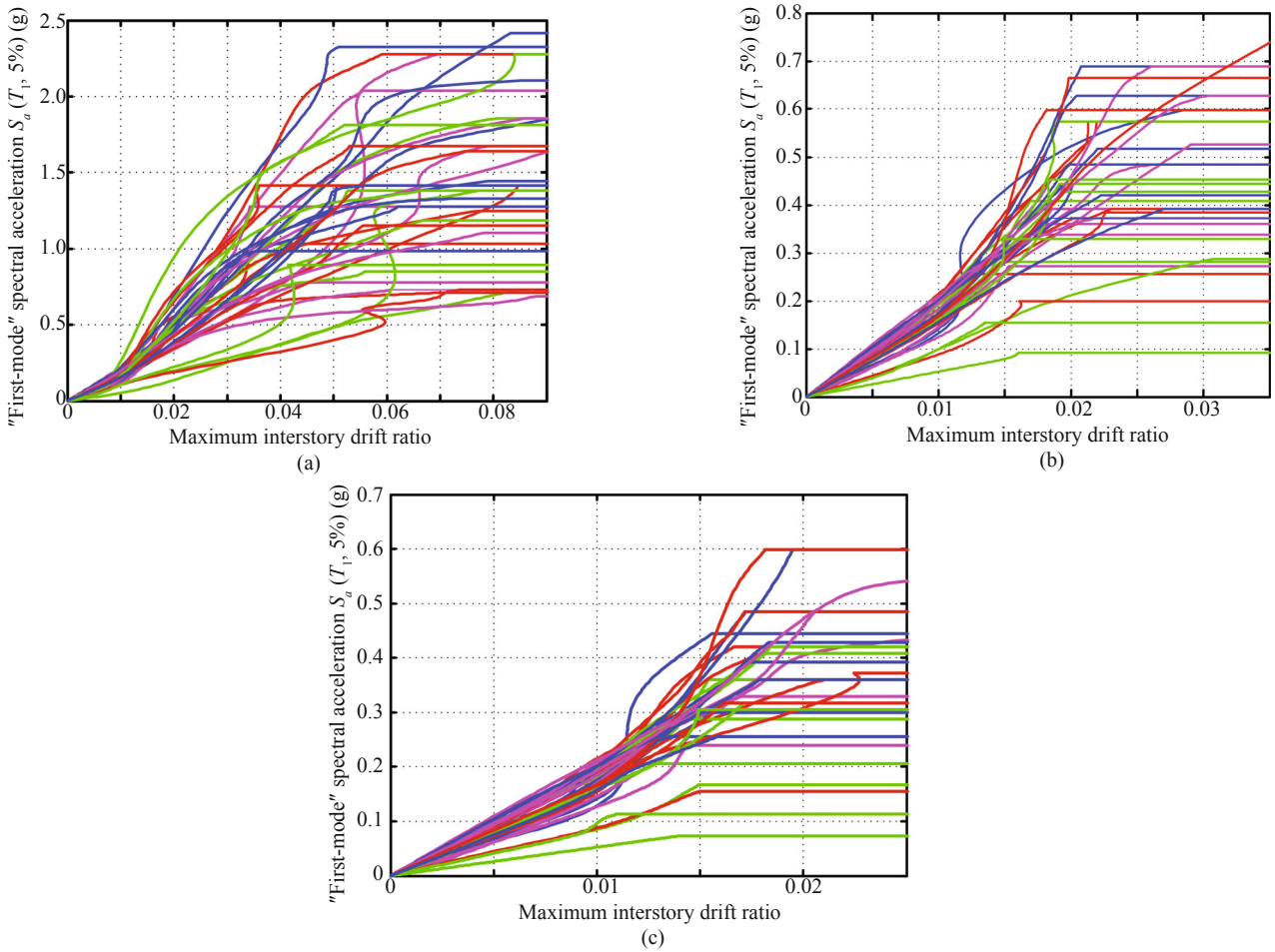

Fig. 10 IDA curves for 5-story building (a) good quality (b) average quality (c) low quality

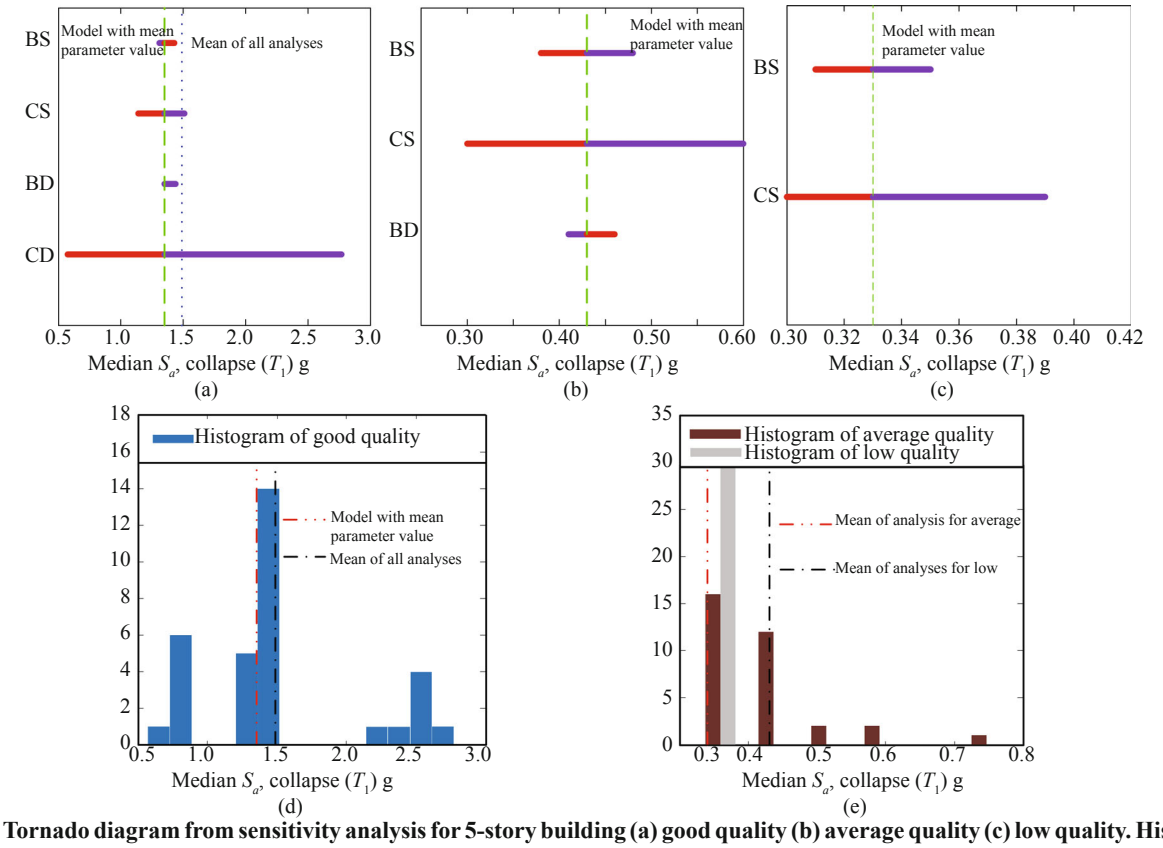

Fig. 11 Tornado diagram from sensitivity analysis for 5-story building (a) good quality (b) average quality (c) low quality. Histogram demonstrating the outcome of 33 sensitivity analysis for (d) good quality (e) average and low quality

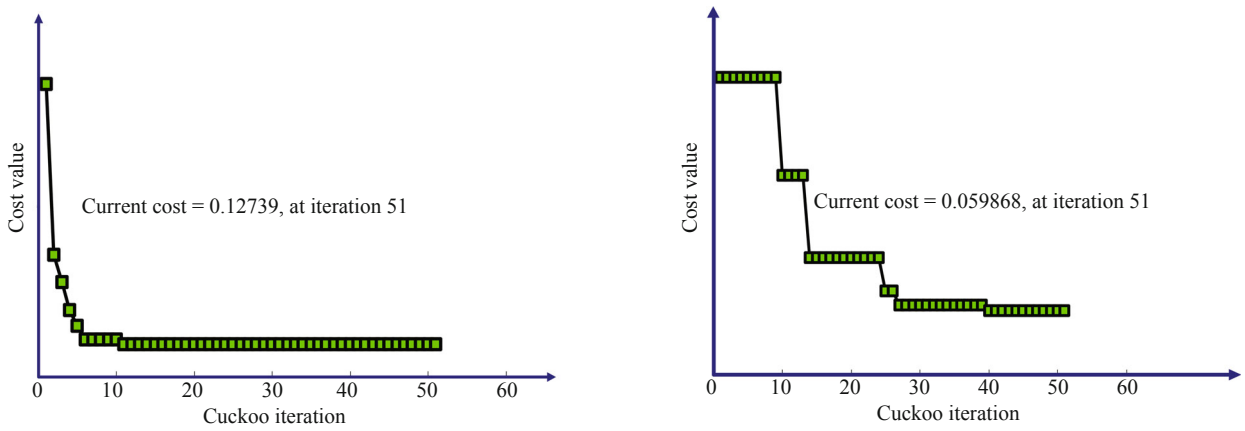

Fig. 12 Best value of COA algorithm

response is large and it is reduced based on quality. In good quality as represented in the tornado diagrams of Fig. 11, CS, BS and BD follow CD which has the largest effect on the mean collapse capacity, and BS has an inverse effect on collapse. For average quality, CS has large effect while CD has no effect in the mean collapse capacity. Finally in low quality, BD and CD have no effect in collapse.

Monte Carlo simulation method has been used to incorporate the effects of modelling uncertainty on the collapse fragility curve as thousands of sets of random variables and IDA analyses of the structure for each realization are necessary. Applying a predefined regression function as response surface in Monte Carlo simulation, the nonlinearities and asymmetries in the relationship between the model random variables and structural response have been represented.

In this approach the first step is to implement the IDA and vertical statistics for computing the two parameters η and β of Eq. (7) which maximize ln (L) by implementing the Cuckoo Search Algorithm (CSA). The parameters applied for the CSA are based on proposed parameters as follows: Number of initial population (numCuckoos = 5), maximum number of eggs for each cuckoo (max Number of Eggs = 4) and the control parameter of egg laying is 5. The optimization procedure is terminated when the number of iterations of the Cuckoo Algorithm reaches 51. A sample of the best value of the objective function is shown in Fig. 12. Vertical statistics is performed for all MQs.

In the next step the functions of the response surface in Eq. (1) are used to predict the means and SD of the fragility curve for a limited number of realizations of the modelling parameters for each quality mentioned in the numerical test section. The response surface function is calculated by the Pinv(x) function in Matlab (2014). For the 5-story example, the surface for the collapse capacity limit state and the mean of the various material qualities for the collapse fragility curves are given by the following Eqs. (14), (15), (16)

$$\begin{aligned}\eta_{\text{Good}} = {} & 0.389 + 0.0277(\text{CD}) + 0.004(\text{BD}) + .0047(\text{CS}) + \\ & 0.00043(\text{BS}) - 0.0086(\text{CD})(\text{BD}) + \\ & 0.0172(\text{CD})(\text{CS}) + 0.0021(\text{CD})(\text{BS}) + \\ & 0.00195(\text{BD})(\text{CS}) + 0.001425(\text{BD})(\text{BS}) + \\ & 2.5\times10^{-5}(\text{CD})(\text{BS}) + 0.00122(\text{CD}^2) - \\ & 0.0029(\text{BD}^2) - 0.00107(\text{CS}^2) - 0.000748(\text{BS}^2)\end{aligned} \tag{14}$$

$$\begin{aligned}\eta_{\text{Ave}} = {} & -0.833 - 0.00213(BD) + 0.129(CS) + \\ & 0.0141(BS) + 0.0065(BD)(CS) + \\ & 0.0057(BD)(BS) + 0.0129(BD^2) + \\ & 0.0286(CS^2) + 0.107(BS^2)\end{aligned} \tag{15}$$

$$\eta_{\text{Low}} = 0.024(\text{CS}) - 0.0006(\text{BS}) + 0.015(\text{CS}^2) + 0.0068(\text{BS}^2) \tag{16}$$

Figure 13 shows the mean effect of the collapse curve in RSM graphically. The best combination of values of the main variables for estimating the mean collapse capacity based on statistical data such as R^2, RMSE and error are given in Fig. 14. It can be seen that for good quality, strength and ductility of columns as well as ductility of beams are desirable while strength of beams is not.

A Sugeno-type fuzzy expert system has been used to consider quality uncertainty. Three rules are considered according to the constant coefficients (one input, three rules, and 30 outputs) that are derived based on the RSM coefficients summarized in Fig. 15. A Gaussian membership function for the index of MQ as input and linear type as output is applied. Also, the weighted average, sum and prod methods are used for defuzzification, aggregation and implication, respectively.

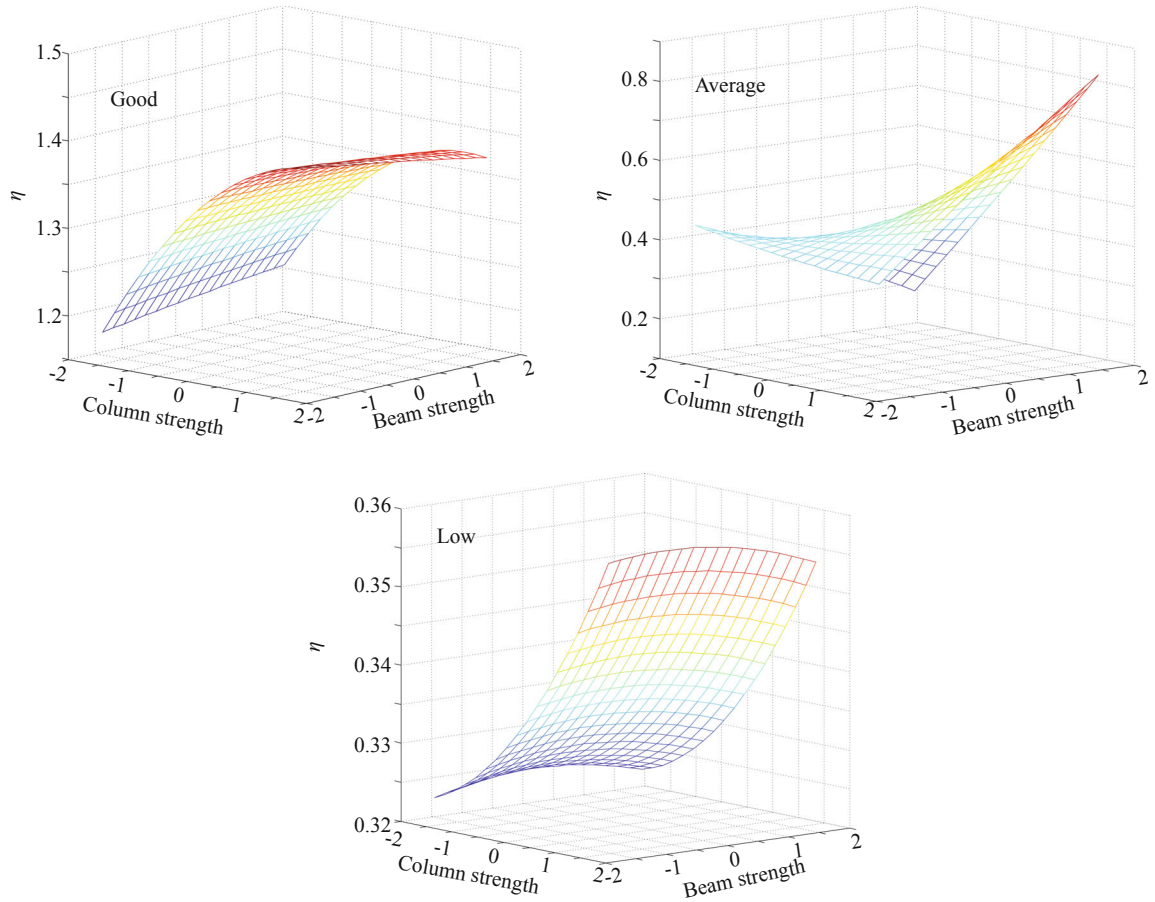

Fig. 13 Response surface curves for collapse limit state in each quality in 5-story

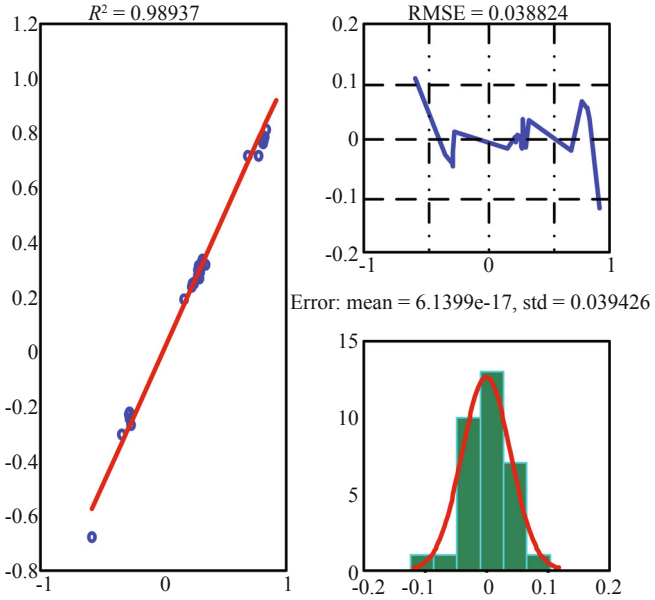

Fig. 14 Statistical value for regression of RSM

Monte Carlo simulation is used for deriving fragility curve involving RTR, modelling and cognitive uncertainty effects. First, 10,000 Monte Carlo realizations are simulated in two parts. One hundred MQs are selected based on a uniform distribution in the interval [1, 3], which are followed by one hundred modelling simulations of the meta variables based on lognormal distribution (η = 0, β = 1). Finally the mean and SD values are obtained for the expected collapse probabilities, which are calculated according to the 100×100 = 10,000 collapse fragilities. Fragility capacity can be evaluated based on the following criteria: (a) mean value of the collapse capacity corresponding to the MCE (maximum considered earthquake acceleration) in the IDA curve, (b) probability of collapse at the MCE intensity, (c) mean annual rate of collapse, as estimated by integrating the fragility curve over the risk curve of a specific site.

Probabilistic hazard analyses have been done for the Tehran region (Zolfaghari, 2014) and the relevant hazard curve which was estimated by fitting the functional form $\beta_0 (S_a)^{\alpha}$ is given in Fig. 16. Based on the hazard curve, the MPE (maximum probable earthquake spectral acceleration) and MCE are 0.477 g, 0.716 g for the 5-story frame, and 0.42 g, 0.62 g for the 10-story frame, respectively. The effects of incorporating modelling uncertainty and material quality for 5 and 10 story sample structures are shown in Fig. 17. Combining the uncertainties into one entity causes the fragility curve to shift to the left and become more widely distributed. In other words, the curve depicts a critical state which becomes more pronounced when the material-related uncertainty comes into play. Neglecting material quality causes underestimation of the collapse fragility probabilities (Table 3). For example, for the 5-story

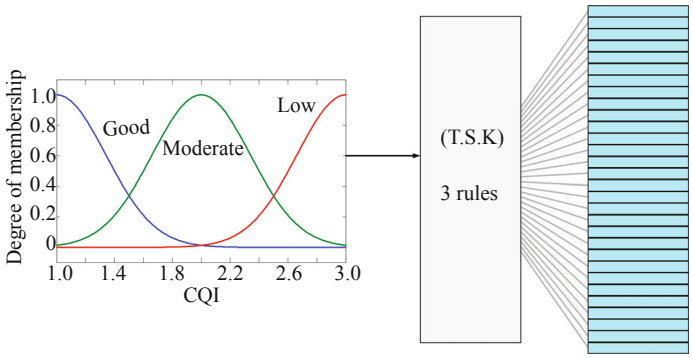

Fig. 15 The structure of TSK system

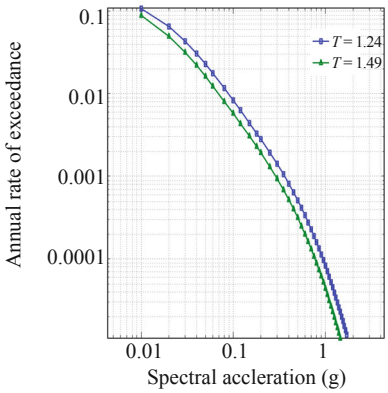

Fig. 16 Seismic hazard curve

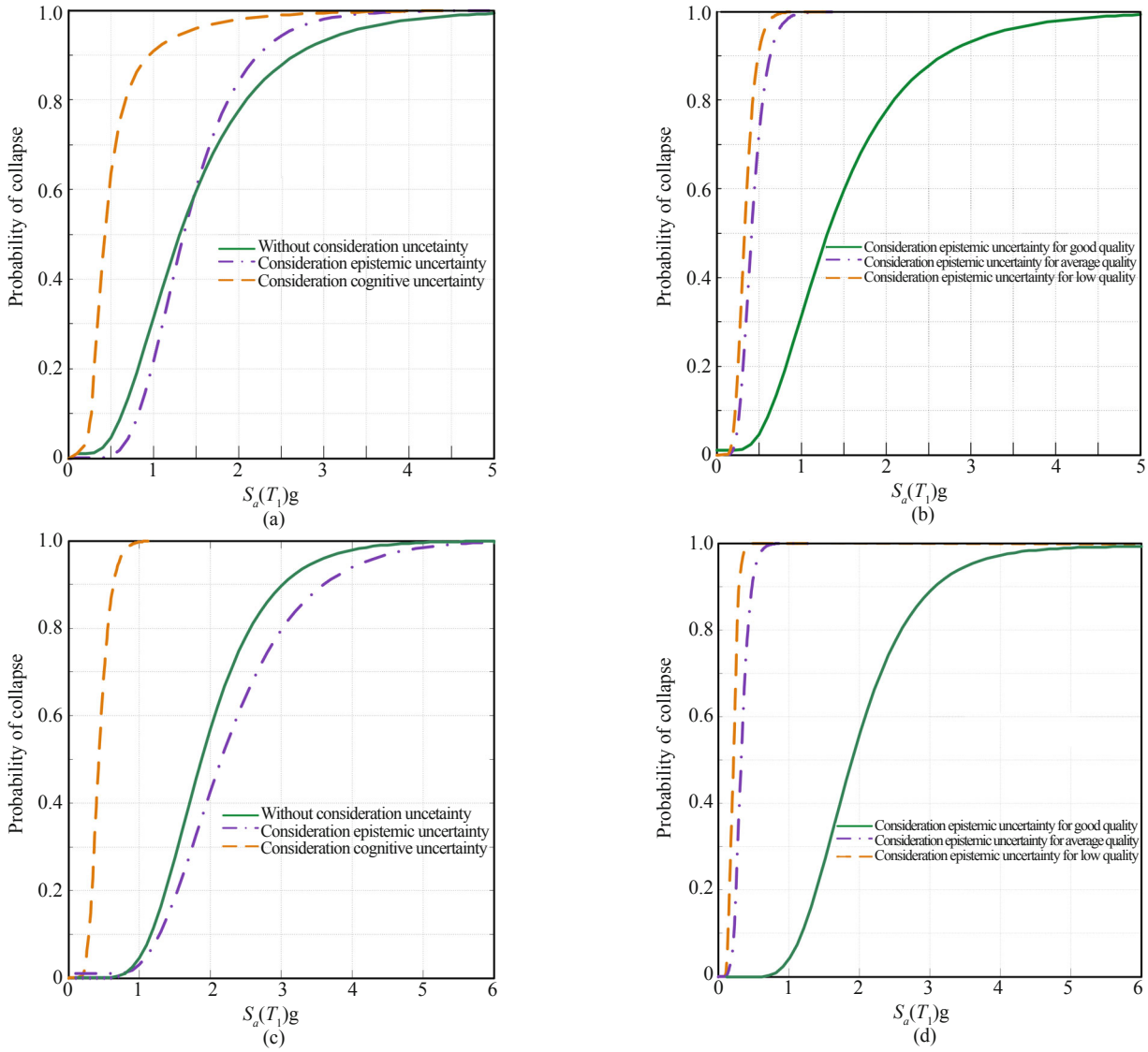

Fig. 17 Collapse fragilities obtained for (a) 5-story building with modelling and MQ quality, (b) 5-story with various quality, (c) 10-story with modelling and MQ quality, (d) 10-story with various quality

structure and considering material quality uncertainty (Fig. 17 (a) and (c)), the mean is decreased to 63% while if it is only modelling uncertainty, the mean is changed by only 3%. In Fig. 17 (d) and (e), fragility curves are obtained by using the RSM for each material quality level separately. It can be observed, MQ uncertainty is the most important factor in deriving fragility curves. According to Table 3, the mean of the fragility curves in low quality for the 10-story structure changes 89%, which is a significant shift in fragility curves.

Table 4 illustrates the probability of collapse in discreet hazard levels (MCE, MPE) and the Mean

Table 3 Variation in collapse fragility curves by uncertainty analysis

	Method	MQ	Change in mean (%)	Change in dispersion (%)
5-ST	RSM	Good	-3	0.5
		Average	-69	13
		Low	-75	18
	TSK	MQ	-64	12
10-ST	RSM	Good	-8	1
		Average	82	19
		Low	89	31
	TSK	MQ	77	18

annual frequency of exceedance (MAFE) in the two sample structures. It can be observed that modelling and MQ uncertainties increase 75%–80% and 40%–50% approximately in MCE and MPE hazard levels, respectively. MAFE is an important factor in risk management and decision making so it can be concluded that material quality is a dominant factor affecting mean annual frequency.

The confidence approach has been applied to incorporate the effects of two uncertainties (modelling and material quality) in estimating the probability of collapse given in IM. By using Fig. 18, one can show the effect of MQ uncertainty on estimating the probability in certain Y confidence level for each sample structure. For example, according to Fig. 18, it can be concluded that for the 5-story building, the collapse probability at MCE and MPE hazard level with the 95 confidence level are 54% and 15%, respectively, (95 confidence means 100%-95% = 5% probability that the actual value of collapse is less than 15%) when considering only modelling uncertainty, and the probability of collapse are 94% and 99% when considering modelling AND quality uncertainty. FEMA guideline requires the probability of collapse for a 50 year period to be smaller than 2% at a confidence level of 95%. Figure 19 shows the MAF variation in the fragility of the 5 and 10 story structures at different confidence levels. It can be seen that the variation is large and the criteria given for the design of the sample structures become unacceptable when all the uncertainties are taken into account.

Table 4 Variation in probability of collapse and mean annual frequency for selected levels of uncertainty

	Method	Uncertainty	P(Collapse|MCE)	P(Collapse|MPE)	MAFE ×(10^{-5})
5-ST	RSM	No consideration	0.0440	0.0050	5.31
		Good	0.1334	0.0465	5.59
		Average	0.9381	0.7200	54.6
		Low	0.9987	0.9154	82.9
	TSK	MQ	0.880	0.58	41.079
10-ST	RSM	No consideration	0.001	0.00016	2.80
		Good	0.020	0.01	3.38
		Average	0.870	0.72	89.6
		Low	100	0.99	195
	TSK	MQ	0.860	0.42	50.5

MQ: incorporation of quality and modelling uncertainty

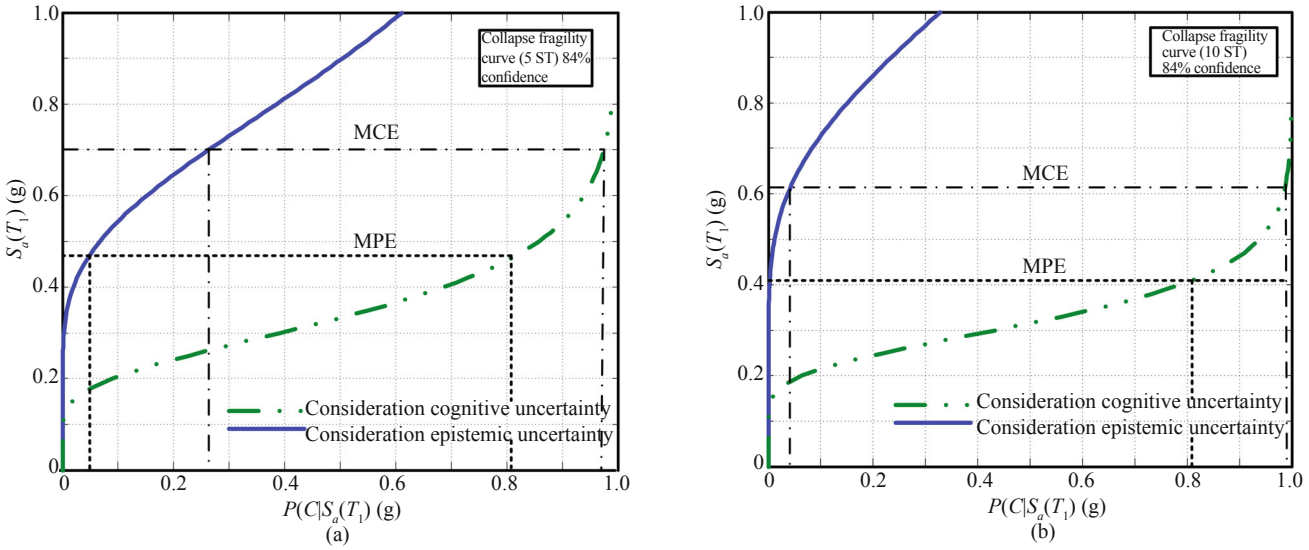

Fig. 18 Fragility curve for collapse safety, considering modelling and material quality uncertainty for (a) 5-story building in 84% confidence (b)10-story in 84% (c) 5-story in 95% (d) 10-story in 95%

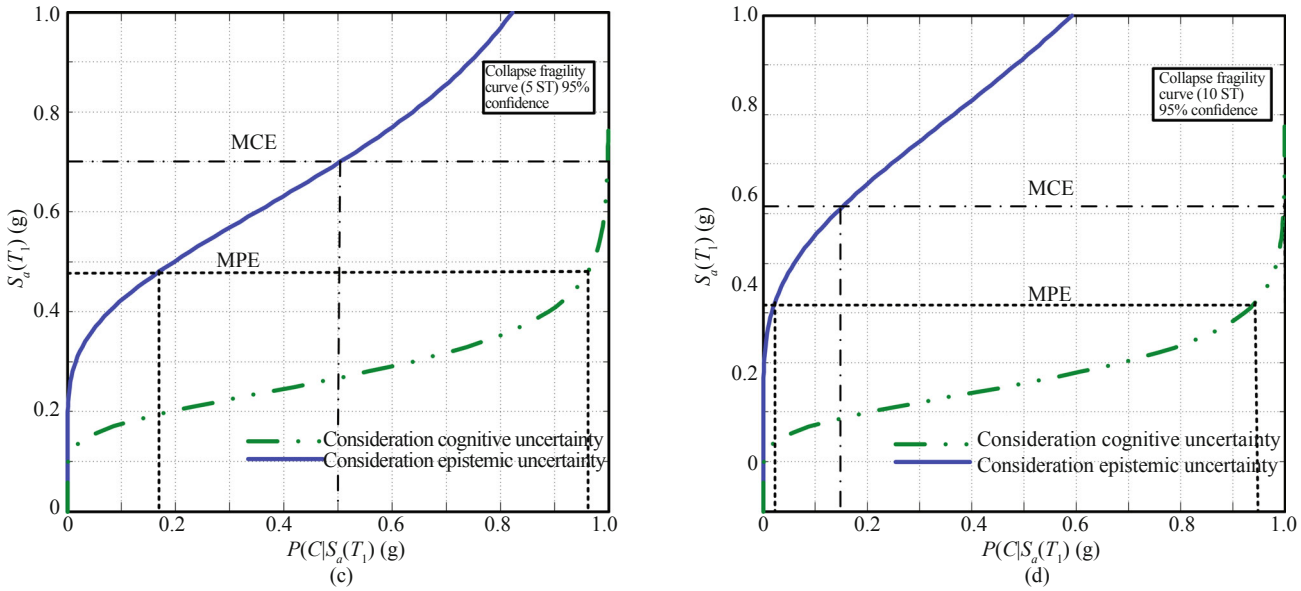

Fig. 18 Continued

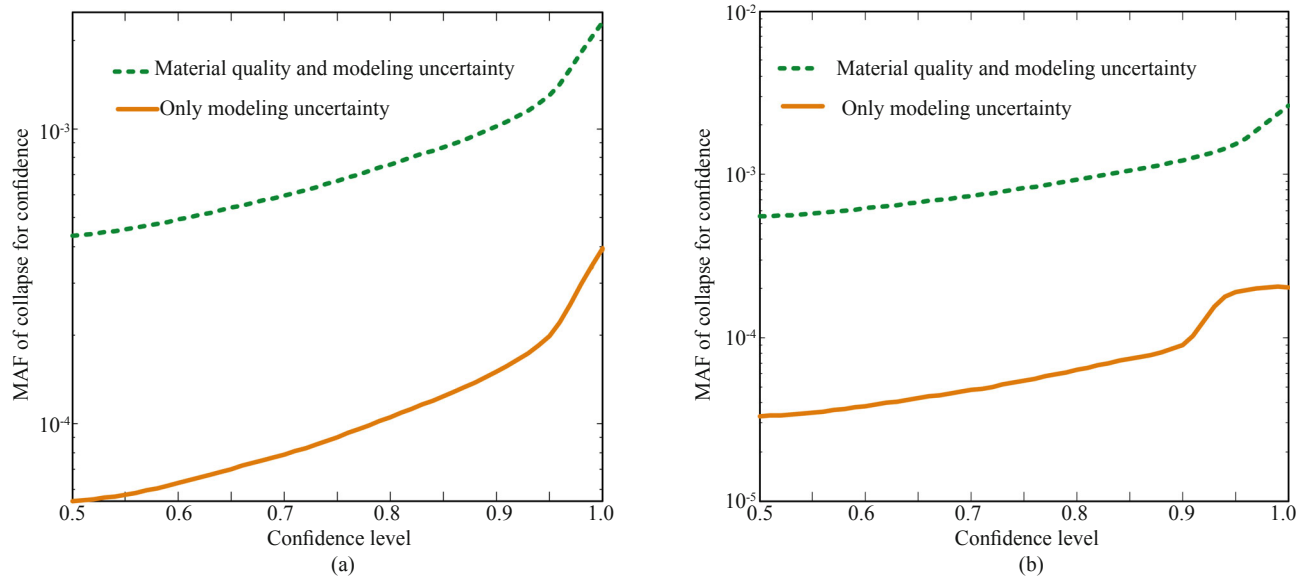

Fig. 19 Effect of confidence level on of MAF with considering comprehensive sources of uncertainty (a) 5-story building (b) 10-story building

4 Conclusion

In this study, the earthquake-related risk of structural collapse has been evaluated with special attention paid to RTR and epistemic (modelling) uncertainties as well as (cognitive) uncertainties related to the quality of the building material. As examples two moment-resisting steel frames, a 5-story and a 10-story, which are designed according to a seismic load corresponding to events with 10% probability of exceedance in 50 years, are analyzed. In order to consider modelling and cognitive uncertainties, modelling parameters are selected from the modified Ibarra–Medina–Krawinkler moment rotation model. A set of 40 records suggested by the k-means clustering algorithm are considered for implementing incremental dynamic analysis for the effect of RTR uncertainty. Then, the mean and SD of the collapse fragility curve which are obtained by IDA and the Cuckoo optimization algorithm are predicted through analytical response functions. Interaction between model variables and structural parameters has been presented as response levels. The response levels qualitatively present the uncertainty in three different levels (good, average, and low). The TSK fuzzy inference system is used to combine these levels into one qualitative uncertainty. Since the sensitivity method is used for predicting the response level, the time taken for the prediction is considerably reduced. The alternative is to use the IDA method to consider all Monte Carlo combinations.

It is observed that almost in all cases disregarding the effect of uncertainties is a conservative result in collapse fragility curve. The dispersion (β_{ln}) in the response fragility increases when modelling and cognitive uncertainties are incorporated. The mean of the curves may be reduced approximately by 70% for cognitive

uncertainty and 10% for modelling uncertainty. This reduction will increase when the number of stories increases. Cognitive uncertainties have greater impact than other uncertainties. Material quality is an important factor in the probability of collapse. Also, while MQ = low, the structure is more brittle. In studying nonlinear variables in the sensitive analysis, it is observed that the effect of ductility in MQ = good is more than other variables while in MQ = low strength is more effective. The effect of uncertainties considered for the sample frames reveal that uncertainties may affect collapse probability significantly when compared with the deterministic approach (not considering epistemic and cognitive uncertainties). Generally it can be concluded that in developing countries where problems of material quality might be observed, cognitive uncertainties should be considered in determining the fragility curve and, hence, the MAF of collapse, which is an important measure for decision making and risk management. Advanced laboratory tests for diagnosing material quality are therefore highly recommended.

References

Cornell CA, Jalayer F, Hamburger RO and Foutch DA (2002), "Probabilistic Basis for 2000 SAC Federal Emergency Management Agency steel moment frame guidelines," *Journal of Structural Engineering*, **128**(4): 526–533.

Dimova SL and Negro P (2006), "Assessment of Seismic Fragility of Structures with Consideration of the Quality of Construction," *Earthquake Spectra*, **22**(4): 909–936.

Ellingwood BR and Kinali K (2009), "Quantifying and Communicating Uncertainty in Seismic Risk Assessment," *Structural Safety*, **31**(2): 179–187.

Erberik MA (2008), "Generation of Fragility Curves for Turkish Masonry Buildings Considering In-plane Failure Modes," *Earthquake Engineering & Structural Dynamics*, **37**(3): 387–405.

Foutch DA and Yun SY (2002), "Modelling of Steel Moment Frames for Seismic Loads," *Journal of Constructional Steel Research*, **58**(5–8): 529–564.

Franchin P, Lupoi A and Pinto PE (2003), "Seismic Fragility of Reinforced Concrete Structures Using a Response Surface Approach," *Journal of Earthquake Engineering*, **7**(sup001): 45–77.

He JN and Wang Z (2011), "Analysis on System Reliability of Steel Framework Structure and Optimal Design," *Applied Mechanics and Materials*, **105–107**: 902–906.

Kappos AJ and Panagopoulos G (2010), "Fragility Curves for Reinforced Concrete Buildings in Greece," *Structure and Infrastructure Engineering*, **6**(1–2): 39–53.

Kircher CA, Reitherman RK, Whitman RV and Arnold C (1997), "Estimation of Earthquake Losses to Buildings," *Earthquake Spectra*, **13**(4): 703–720.

Kiureghian AD and Ditlevsen O (2009), "Aleatory or epistemic? Does It Matter?," *Structural Safety*, **31**(2): 105–112.

Kramer SL (1996), *Geotechnical Earthquake Engineering*, Prentice Hall, Upper Saddle River, N.J.

Li Q and Ellingwood BR (2008), "Damage Inspection and Vulnerability Analysis of Existing Buildings with Steel Moment-resisting Frames," *Engineering Structures*, **30**(2): 338–351.

Liel AB, Haselton CB, Deierlein GG and Baker JW (2009), "Incorporating Modelling Uncertainties in the Assessment of Seismic Collapse Risk of Buildings," *Structural Safety*, **31**(2): 197–211.

Lignos D (2008), *Sidesway Collapse of Deteriorating Structural Systems under Seismic Excitations*, ProQuest.

Lloyd SP (1982), "Least Squares Quantization in PCM," *IEEE Transactions on Information Theory*, **28**(2)*:* 129–137.

Matlab (2014a), *The Language of Technical Computing, Version 8.3*, MathWorks.

Mitropoulou CC and Papadrakakis M (2011), "Developing Fragility Curves Based on Neural Network IDA Predictions," *Engineering Structures*, **33**(12): 3409–3421.

Möller B, Graf W and Beer M (2003), "Safety Assessment of Structures in View of Fuzzy Randomness," *Computers& Structures*, **81**(15): 1567–1582.

OpenSEES (2006), *Open System for Earthquake Engineering Simulation*, Pacific Earthquake Engineering Research Centre, University of California, Berkeley, (Release 2. 4. 2).

Pinto P, Giannini R and Franchin P (2007), "Seismic Reliability Analysis of Structures," *Earthquake Engineering & Structural Dynamics*, **36**(13): 2081–2081.

Rajabioun R (2011), "Cuckoo Optimization Algorithm," *Applied Soft Computing*, **11**(8): 5508–5518.

Rajeev P and Tesfamariam S (2012), "Seismic Fragilities for Reinforced Concrete Buildings with Consideration of Irregularities," *Structural Safety*, **39**: 1–13.

Rossetto T and Elnashai A (2005), "A New Analytical Procedure for the Derivation of Displacement-based Vulnerability Curves for Populations of RC Structures," *Engineering Structures*, **27**: 397–409.

Schotanus MIJ, Franchin P and Lupoi A (2004), "Seismic Fragility Analysis of 3D Structures," *Structural Safety*, **26**: 421–441.

Seo J and Linzell DG (2012), "Horizontally Curved Steel Bridge Seismic Vulnerability Assessment," *Engineering Structures*, **34**: 21–32.

Seo J and Linzell DG (2013), "Use of Response Surface Metamodels to Generate System Level Fragilities for Existing Curved Steel Bridges," *Engineering Structures*, **52**: 642–653.

Shinozuka M, Feng MQ, Lee J and Naganuma T (2000), "Statistical Analysis of Fragility Curves," *Journal of Engineering Mechanics*, ASEC, **126**(12): 1224–1231.

Shokri-Ghaleh H and Alfi A (2014), "Optimal Synchronization of Teleoperation Systems via Cuckoo

Optimization Algorithm," *Nonlinear Dynamics*, **78**(4): 2359–2376.

Siler W and Buckley JJ (2005), *Fuzzy Expert Systems and Fuzzy Reasoning*, John Wiley & Sons.

Standard No. 2800 (2007), *Iranian Code of Practice for Seismic Resistant Design of Buildings*, Building and Housing Research Center, 3rd Edition, Iran.

Sugeno M (1985), "An Introduction Survey of Fuzzy Control," *Information Sciences*, **36**(1-2): 59–83.

Vamvatsikos D (2007), "Performing Incremental Dynamic Analysis in Parallel Using Computer Clusters," *In Proceedings of COMPDYN2007 Conference on Computational Methods in Structural Dynamics and Earthquake Engineering,* Rethymno, Greece.

Zareian F, Krawinkler H, Ibarra L and Lignos D (2009), "Basic Concepts and Performance Measures in Prediction of Collapse of Buildings under Earthquake Ground Motions," *The Structural Design of Tall and Special Buildings*, **19**(1-2): 167–181.

Zolfaghari MR (2014), "Development of a Synthetically Generated Earthquake Catalogue towards Assessment of Probabilistic Seismic Hazard for Tehran," *Natural Hazards*, **76**(1): 497–514.

Appendix

The suit of 40 ground motion records.

No	Year	Earthquake	M_w	Mech.[1]	Station	GM Characteristics	Dist.[2] (km)	PGA (g)	I_A (m/s)	I_C	CAV
1	1994	Northridge	6.7	RN	Leona Valley #2	Far-Fault	37.2	0.063	0.06252	0.00676	216.82
2	1994	Northridge	6.7	RN	Lake Hughes #1	Far-Fault	89.67	0.077	0.10962	0.0103	301.778
3	1994	Northridge	6.7	RN	LA, Hollywood Stor FF	Far-Fault	114.62	0.358	2.00474	0.08616	1185.35
4	1994	Northridge	6.7	RN	LA, Centinela St.	Far-Fault	31.53	0.322	0.99385	0.0547	799.35
5	1989	Loma Prieta	6.9	RO	WAHO	Far-Fault	17.50	0.672	6.27237	0.22791	2025.38
6	1989	Loma Prieta	6.9	RO	Halls Valley	Far-Fault	30.50	0.102	0.24847	0.018	467.845
7	1989	Loma Prieta	6.9	RO	Agnews State Hospital	Far-Fault	24.60	0.159	0.37439	0.02447	625.39
8	1989	Loma Prieta	6.9	RO	Anderson Dam (Downstream)	Far-Fault	4.40	0.24	0.80107	0.0434	721.197
9	1979	Imperial Valley	6.5	SS	Chihuahua	Far-Fault	8.4	0.254	1.18662	0.05813	1110.14
10	1979	Imperial Valley	6.5	SS	Bonds Corner	Far-Fault	4.01	0.588	3.90282	0.14418	1471.17
11	1987	Superstition Hills	6.7	SS	El Centro Imp. Co Cent	Far-Fault	18.5	0.258	0.67456	0.03806	814.968
12	1987	Superstition Hills	6.7	SS	Plaster City	Far-Fault	22.5	0.121	0.29862	0.02395	447.696
13	1987	Superstition Hills	6.7	SS	Brawley Airport	Far-Fault	29.91	0.116	0.24856	0.02091	427.309
14	1987	Superstition Hills	6.7	SS	Superstition Mtn Camera	Far-Fault	6.56	0.894	6.02742	0.22789	1908.88
15	1987	Superstition Hills	6.7	SS	Westmorland Fire Sta	Far-Fault	13.47	0.211	1.17613	0.05774	1073.18
16	1983	Coalinga	6.4	RN	Parkfield — Cholame 2WA	Far-Fault	44.72	0.114	0.19526	0.01502	422.411
17	1983	Coalinga	6.4	RN	Parkfield — Fault Zone 14	Far-Fault	29.48	0.274	0.88032	0.04647	844.768
18	1983	Coalinga	6.4	RN	Parkfield — Gold Hill 3W	Far-Fault	39.12	0.122	0.15312	0.01252	330.881
19	1983	Coalinga	6.4	RN	Parkfield — Stone Corral 3E	Far-Fault	34.00	0.106	0.12442	0.01217	270.909
20	1983	Coalinga	6.4	RN	Pleasant Valley P.P. — yard	Far-Fault	8.41	0.551	3.8457	0.14045	1506.25
21	1987	Whittier Narrows	6	RO	Alhambra—Fremont School	Far-Fault	14.66	0.413	0.87457	0.04624	593.004
22	1987	Whittier Narrows	6	RO	LA—Hollywood Stor FF	Far-Fault	24.08	0.124	0.15938	0.0129	351.832
23	1987	Whittier Narrows	6	RO	Altadena—Eaton Canyon	Far-Fault	19.52	0.151	0.18627	0.0145	309.673
24	1987	Whittier Narrows	6	RO	Brea Dam (Downstream)	Far-Fault	23.99	0.313	0.4169	0.02852	408.27
25	1979	Coyote Lake	5.7	SS	Gilroy Array #1	Far-Fault	10.67	0.132	0.07987	0.00849	170.129
26	1979	Coyote Lake	5.7	SS	Coyote Lake Dam (SW Abut)	Far-Fault	6.13	0.279	0.35919	0.02575	338.147
27	1979	Coyote Lake	5.7	SS	Gilroy Array #2	Far-Fault	9.02	0.339	0.5126	0.03422	399.466
28	1979	Coyote Lake	5.7	SS	Gilroy Array #6	Far-Fault	3.11	0.316	0.6798	0.0422	421.295
29	1992	Cape Mendocino	7.1	RN	Eureka—Myrtle & West	Far-Fault	41.97	0.178	0.33065	0.02177	579.139
30	1992	Cape Mendocino	7.1	RN	Fortuna—Fortuna Blvd	Far-Fault	19.95	0.114	0.23911	0.01707	491.474
31	1992	Cape Mendocino	7.1	RN	Petrolia	Far-Fault	8.18	0.662	3.82072	0.14349	1456.08
32	1981	Westmorland	5.8	SS	Brawley Airport	Far-Fault	15.57	0.171	0.18547	0.01574	303.306
33	1981	Westmorland	5.8	SS	Niland Fire Station	Far-Fault	15.5	0.176	0.17397	0.01377	339.247
34	1981	Westmorland	5.8	SS	Parachute Test Site	Far-Fault	16.81	0.155	0.49073	0.02998	670.89
35	1981	Westmorland	5.8	SS	Salton Sea Wildlife Ref	Far-Fault	8.15	0.176	0.51288	0.03366	542.232
36	1992	Landers	7.3	SS	Desert Hot Springs	Far-Fault	21.98	0.154	0.6776	0.03612	1050.99
37	1992	Landers	7.3	SS	Amboy	Far-Fault	69.17	0.146	0.75468	0.03916	1064.58
38	1992	Landers	7.3	SS	Lucerne	Far-Fault	3.71	0.789	6.58484	0.20068	2483.47
39	1992	Landers	7.3	SS	Joshua Tree	Far-Fault	11.34	0.284	2.34815	0.09472	1746.59
40	1992	Landers	7.3	SS	Morongo Valley	Far-Fault	17.58	0.188	0.95827	0.04305	1272.15

1 Faulting Mechanism = TH: Thrust; REV: Reverse; SS: Strike-slip; OB: Oblique; RN: Reverse-Normal; RO: Reverse-Oblique; NO: Normal-Oblique

2 Closest distance to fault rupture (i.e., r_{jb})